JMME. Vol. 10 September 2015 *ISSN: 2006-1919*
pp. 18-32

A NEW COMBINATORIAL APPROACH TO PROPERTY-DRIVEN DESIGN OF Ti ALLOYS FOR BIOMEDICAL APPLICATIONS

Paul S. Nnamchi, Boniface A. Okorie, and Camillus S. Obayi

Department of Metallurgical and Materials Engineering,
University of Nigeria, Nsukka, Nigeria.
Tel.: +2347064278906; +447928921079.
E-mail addresses: paul.nnamchi@unn.edu.ng; nnamchi.paul@gmail.com.

ABSTRACT
Ti and Ti based alloys containing nontoxic elements, such as Nb, Mo, Ta, and Zr have been proposed as prospective candidates for biomedical applications, due to their excellent corrosion resistance, biocompatibility, high strength, toughness and wear resistance. However, stress shielding has become a major setback to their application. When elastically soft bone tissue (~E=20-40GPa) is replaced by a stiffer implant, the implant takes over a considerable amount of the load, shielding the surrounding parts of the skeleton. Reducing the physiological loads on the bone induces re-sorption processes that give rise to a drop in bone density, mineralization state and strength. Stress shielding can finally promote contact loosening, implant failure, or debris-induced infections. For this, the aim of this study is to develop a new biomaterial to use in the load transfer implant field. An ab initio theoretical calculation was used to couple elastic properties from homogenised multiphase elastic parameters for the design of new Ti-Mo-Nb-Zr alloys with bone matching modulus. The agreement between the predictions and detailed experimental characterization, sheds light on the decisive influence of the multi-phase character of the polycrystalline composites on their structural and mechanical properties. An attempt is also made to highlight the influence of heat treatment and cold work in enhancing the modulus of the alloys. The study shows that the novel combinatorial approach can be highly beneficial as it may lead to something of a breakthrough with respect to reducing the Young's modulus of metallic biomaterials, which is pertinent to preventing stress shielding and bone resorption in orthopedic implants.

Keywords: *Ti based alloys; Young's modulus, phase stability; ab initio; elastic modulus; elastic constant; biomedical implant application.*

1.0 INTRODUCTION
Health care has become one of the front burner research fields of this century owing to the dramatic increase in the number of people affected by various diseases. Health care costs and the urgent requirement for biomaterials have placed enormous pressure on government funding agencies and researchers to develop cost effective, appropriate biomaterials to treat various diseases and to regenerate or replace dysfunctional tissues or organs [1]. Thus, various funding organization have allocated considerable funding for the development of the next generation of metallic and associated biomaterials.

Amongst metallic biomaterials, titanium is generally considered as one of the most biocompatible and corrosion resistant metals available for biomedical or clinical applications. From 1951, when Leventhal [2] first published an article on the orthopedic application of this metal until now, there has been a thrust towards new developments in the manufacturing and use of this metal and its varieties of alloys in orthopedic applications and other clinical related activities. Beginning with commercially pure Ti, and then to Ti-6Al-4V alloy, today's state of the art β-Ti alloys have been added to the list. There is a range of materials and devices based on titanium, which are available for a variety of medical applications. These alloys are known to possess many attractive properties such as excellent corrosion resistance in biological environment, superior biocompatibility, high specific strength and wear resistance and provide adequate mechanical properties when compared to other metallic biomaterials [3.4]. However, stress shielding effect due to high elastic stiffness comparable to that of human bone has become a major setback. When elastically soft bone tissue is replaced by a stiffer implant, the implant takes over a considerable

amount of the load, shielding the surrounding parts of the skeleton. Reducing the physiological loads on the bone induces re-sorption processes that give rise to a drop in bone density, mineralization state and strength [25]. Stress shielding can finally promote contact loosening, implant failure, or debris-induced infections. Therefore, it is of great importance that the elastic mismatch between the bone replacement material and existing bone be minimized in metallic biomaterials intended for orthopaedic application.

Over the past few years, significant effort has been devoted to develop bone matching Ti-based alloys, and a few of them have already been implemented into biomedical applications [5]. They usually contain multiple non-toxic alloying elements, such as Mo, Nb, Ta, and Zr, which are preferred as β stabilizers or/and which play the key role in decreasing the Young's modulus [6-7]. To design these multi-component alloys, several methods have been proposed like d-electrons concept [9] and Mo-equivalence method [10]. However, it is difficult to determine the optimum alloy composition with sufficiently metastable β phase and enough low modulus which is generally achieved by multiple alloying of simple binary alloys. To design novel Ti-based alloys with desirable properties, it is necessary to develop a theoretical framework in selecting suitable alloying elements.

In recent years, computational material design based on first principles quantum mechanical methods have emerged as an important cost effective tool to design material properties [11,12]. Biocompatible Ti alloys have been investigated experimentally, and by theoretical studies, but such efforts notwithstanding, a review of the literature indicates that multicomponent Ti-Mo alloys have received considerably little attention [13,14], even though the Ti-Mo system has proved to be a good substitute for developing absolutely safe Ni-free biomedical Ti alloys due to their being non-toxic and non-allergic elements. Nevertheless, the Young's moduli of the Ti-Mo alloy systems reported so far are not low enough [15-17], and there has been little research effort into the Young's moduli of multicomponent metastable β-phase Ti-Mo alloys. Moreover, a central theoretical framework of low modulus determining factors in alloys remains elusive and our understanding is not nearly as sharp as it should be in the area. A relatively good understanding could be obtained by density functional theory, which has been proved to be a useful tool to reveal natural properties of many compounds from atomic scale considerations [18, 19].

Generally speaking, if the content of β phase stabilizing elements (e.g. Mo, Nb and Zr) doesn't exceed a critical amount in the Ti-X binary alloys, three kinds of metastable phase transformations can occur depending on process techniques. The occurrence of β phase would depend on the competition amongst different phases. Therefore, in titanium alloy design for low elastic modulus, a consideration of phase homogenization is important as it can yield results close to experimental results. In this paper, the authors have attempted to calculate by *ab initio* method the integral elastic response of multi-phase polycrystalline aggregates based on multiple scattering in the Ti-6Mo-xNb-xZr alloys, with respect to thermodynamic phase stability, and on structural and mechanical properties, including Young's modulus.

2.0 CALCULATION METHOD

Our calculations were carried out using the Cambridge Serial Total Energy Package code (CASTEP) [22, 23). In this code, the Kohn-Sham [31] single electron equation model was used to calculate the fundamental eigenvalue [25]. To minimise the basis set, Perdew, Burke and Ernzerhof (PBE) formalism [32] was used to describe the real electronic functions while the CASTEP code was used for calculations due to its computational efficiency. The pseudo-potential approximation was presented by replacing the nucleus and the core electrons by an effective potential [25].The exchange correlation is treated using the generalised-gradient approximation (GGA) of Perdew, Burke and Ernzerhof (PBE) formalism [32], because of its accuracy in describing the bulk

properties of many materials, and because it is flexible enough to describe the random distribution of the impurity atoms in the Ti lattice [28]. The PBE functional is designed to reproduce closely the PW91 results [26], but the PBE formulation is more robust to guarantee a high level of convergence, cut-off energy of 500 eV and smearing of 0.1 eV electron levels.

For each structure, tests were carried out using different k-point meshes to ensure absolute convergence of the total energy to within a range better than 1.0 meV/atom. Through this study, we calculated the total energies as a function of volume while optimising unit cell-external degree(s) of freedom (i.e. the unit-cell shape) and unit cell-internal degree(s) of freedom (i.e. Wyckoff positions) as permitted by the space-group symmetry of the crystal structure. Such structural optimisations were iterated until the Hellman–Feynman forces were less than 4 meV/Å in magnitude, ensuring a convergence of the energy with respect to the structural degrees of freedom to better than 1 meV/atom (~0.1 kJ/mol). In addition, all calculations were performed using the ‘‘accurate’’ setting within CASTEP code to avoid wrap-around errors. With the chosen plane-wave cut-off and k-point sampling, the reported formation energies are estimated to be converged to a precision better than 2 meV/atom.

In addition to the optimization, we performed a random distribution of the chemical species over the sites of the structures by replacing Ti atoms with Mo, Zr or Nb atoms, but this had no effect on the system. Nb and Zr atoms are added to binary Ti-6Mo supercell consisting of sixty four atoms to attain an average of 0, 6, 6, 5 and 4 at. % of Nb and 6, 0, 2, 3 and 4at. % of Zr, respectively, (See Fig. 1 and 2).

The stoichiometry was chosen for many reasons. (i) In our previous work on binary Ti–Mo-based alloys, we have seen that some important elastic responses (such as Young’s modulus) are sensitive functions of composition, requiring Mo contents lower than a critical level of about 6-8 at. %, thus requiring composition of around the least stable β phase in the Ti-Mo alloy system [5]. (ii) Further, it has been shown earlier that the composition of the least stable β phase alloy, βc, correlates in some ways with the emergence of many unique properties, such as non-linear superelasticity and very low work hardening rate [28]. (iii) From the view point of memory and time cost, a traceable size of the stoichiometry was chosen. (iv) In line with previous work elsewhere, the stoichiometry was held constant to provide an atom-atom comparison of the relative potency of different substitutional solutes to enhance β stability; and finally (v) holding the symmetry and size of the supercell constant promotes maximum cancellation of numerical errors.

2.1 Calculation details

2.1.1 Thermodynamic phase stability

Material design for biomedical application or implant usage is essentially a multi-criteria optimisation constrained by (1) biocompatibility of the alloy elements, and (ii) possession of elastic modulus that is as bone matching as possible. For this perspective, a detailed insight of how alloy composition affects the stability of β-phase is needed to tailor the Young’s modulus. In the present work, we studied the effect of Zr and Nb micro-additions (biocompatible elements) on the relative stability of the Ti-6Mo alloy (i.e. initial least stable β composition) by ab initio calculation. The formation energy of an alloy has been described by several authors as one of the most important quantities that can be used to reveal thermodynamic stability and understand metallurgical trends in the properties of an alloy.

In the present work, the formation energies of the (omega) ω, (hexagonal) α, (orthorhombic) α′′and (bcc) β phases for the Ti-6Mo-xNb-xZr alloys were calculated according to Eqn.1 below.

$$\mathrm{E}_{\mathrm{FM}}^{((Ti_xMo_6+U))} = \frac{E_{tot}^{bulk}\left((Ti_xMo_6+U)\right)}{\sum_i N} - \kappa\mu^{((Ti_xMo_6+U))}\left(\mathrm{E}_{\mathrm{N(i=1)}}^{(Ti_xMo_6+U+G)} - (1-\kappa).\mu^{((Ti_xMo_6))}(E_{N(i=1)}^{(Ti_xMo_6)})\right) \quad (1)$$

Here, *U* represents one or combined atoms of Zr and Nb; N is the total number of atoms per

supercell; $E_{tot}^{bulk}(Ti_xMo_6 + U)$ is the first principle calculated total energies of the respective alloys; μ is the chemical potential of the alloys in corresponding bulk phase, and κ is the alloy composition. In the above definition (Eqn.1), the alloy is thermodynamically stable for $E_F^0 < 0$. Therefore, from the stand point of thermodynamics, lower formation energy implies better stability of a particular crystal structure over another.

Similarly, the cohesive energy E_c, of a single metal compound, defined as the work needed to decompose the crystal into single free atoms [23] and expressed according to Eqn. (2) can be used to measure or complement the structural stability determined by the formation energy.

$$E_c = 1/n + m + \cdots . (E_{tot} - nE_{atom}^{A} - nE_{atom}^{B} + \cdots .) \quad (2)$$

Here, $nE_{atom}^{A} - nE_{atom}^{B}$ are the energy per atom of A and B compounds in an isolated state.

2.1.2 Calculation of polycrystalline elastic parameters

In our previous work on binary Ti–Mo-based alloys [5], we have seen that binary Ti-6Mo alloy exhibits two structures consisting of cubic and orthorhombic phase fractions. Therefore, the subset of the supercells or cubic and orthorhombic symmetries consisting of three (C_{11}, C_{12}, C_{44}) and nine (C_{11}, C_{12}, C_{13}, C_{22}, C_{23}, C_{33}, C_{44}, C_{55}, C_{66}) elastic constants, respectively, were calculated by employing the methodology of the integral elastic response of multi-phase polycrystalline aggregates as explained in [29, 30], which was originally applied by Zeller and Dederichs [31] to determine elastic properties of single phase polycrystals with cubic symmetry. The concept was extended to determine the multiphase composites of hexagonal α phase and bcc β- phase in binary Ti-Nb and Ti-Mo alloys by M. Friak et al [34]. Here, we apply this criterion to calculate (a) the elastic properties of homogenized components of orthorhombic martensitic α′′ phase and the bcc β-phase and (b) the volume fractions in multicomponent Ti-6Mo –xNb-xZr alloys. For materials with orthorhombic symmetry, Eqns. (21) and (22) in [34] comes to Eqns. (3) and (4), respectively:

$$15\tau_{44} = \frac{a-b+\beta(2d-2c-e)+3\gamma(d-c+e)+\eta\beta\Delta'}{1-\alpha\beta-9\gamma(K_v-\tilde{B}_0)+\beta(\beta+2\gamma)(c-d)-2e\beta\gamma-\frac{1}{3}\eta\beta^2\Delta''} + 3\left(\frac{C_{44}-\tilde{\mu}^O}{1-2k(C_{44}-\tilde{\mu}^O)} + \frac{C_{55}-\tilde{\mu}^O}{1-2k(C_{55}-\tilde{\mu}^O)} + \frac{C_{66}-\tilde{\mu}^O}{1-2\beta(C_{66}-\tilde{\mu}^O)}\right) \quad (3)$$

$$\tau_{11} + 2\tau_{12} = \frac{9\left(K_v-\tilde{B}^0\right)+2\beta(d-c+e)+3\beta^2\Delta'}{3\left[1-\alpha\beta-9\gamma(K_V-\tilde{B}^0)+\beta(\beta+2\gamma)(c-d)-2e\beta\gamma-\frac{1\eta\beta^2\Delta'}{3}\right]} \quad (4)$$

Here, G and B replace μ^* and B^* in the equations for β, η, and Δ'. As soon as G and B have been determined, the homogenized polycrystalline Young's modulus (E) and Poisson's ratio (ν) can be obtained using standard elastic relationships: The homogenised polycrystalline Young's modulus is calculated using:

$$E = \frac{9BG}{3B+G} \quad (5)$$

and the homogenized polycrystalline Poisson's ratio using:

$$\nu = \frac{3B-2G}{3(2B+G)} \quad (6)$$

2.2 Experimental verification Methods

In order to compare the predictions with experimental data, Ti-6Al-4V and the new multicomponent Ti-Mo alloys, namely, Ti-6Mo-6Nb, Ti-6Mo-6Zr, Ti-6Mo-6Nb-2Zr, Ti-6Mo-5Nb-3Zr, Ti-6Mo-4Nb-4Zr, (all in at. %) were melted, cast and homogenized at T = 1200 ◦C. Characterization was done with X-ray Bragg diffraction method in conjunction with EDXRF analyses. Differential thermal analysis (DTA) was used to identify the changes in the transition temperature, while, the Young's modulus of the samples was measured by ultrasonic method on an ultrasonic velocity gauge, Olympus 62, UK. A normal incident probe (model M110, 5MHz) and a shear probe (model V221, 5MHz) were used for the measurement of normal and shear velocities of the wave, respectively. The density of the samples was measured on an automatic density meter; for at least five times. The relationships between ultrasonic velocity and the elastic properties of materials are given below [24-29]. Young's modulus (E) is expressed as:

$$E = \frac{\rho V_S^2(3V_L^2-4V_S^2)}{V_L^2-V_S^2} \quad (7)$$

Shear modulus (G) is the ratio of shearing stress τ to shearing strain γ within the proportional limit of a material and is expressed as:

$$G = \rho V_S^2 \quad (8)$$

Poisson's ratio υ is the ratio of transverse contraction strain to longitudinal extension strain in the direction of stretching force, and is expressed as:

$$\upsilon = \frac{\left(\frac{1}{2}\right)(V_L^2-2V_S^2)}{V_L^2-V_S^2} \quad (9)$$

In the above set of equations, *Vl* and *Vs* are the ultrasonic longitudinal and shear wave velocities, respectively, and ρ is the density of the material.

3. RESULTS AND DISCUSSION

3.1. Structure information and thermodynamic phase stability: theory

In all the six variants in Table 1, Ti-Mo alloys are generally characterized as disordered in the ground state and a random distribution of the chemical species (namely Ti, Mo, Nb and Zr) over the sites of the β (bcc), ω (omega), α (hexagonal) or α´´ (orthorhombic) lattices is assumed. The structure of the alloys is approximated by a large supercell whose sites are occupied such as to minimize the total energy of the system (See Fig. 1 and 2).

Table 1: **Theoretically predicted structural parameters and thermodynamic properties of the multicomponent Ti-6Mo-x-Nb-XZr alloys**

	Formation Energy, E_{Fm} (MeV) of the phases				a,(Å)	E_c(MeV)
Compounds	Im3m(β)	P6/mmm (α)	*Cmcm* (α´´)	p$\bar{3}$m1(ω)	(Cal/Exp.)	
Ti-6Mo	-48	-28	-41	-35	3.24/3.29	-6.15
Ti-6Mo-6Zr	-55.3	-35.3	-45.3	-45.1	3.2/3.31	-5.38
Ti-6Mo-6Nb	-84.1	-44.1	-67.1	-47.1	3.11/3.20	-12.6
Ti-6Mo-6Nb-2Zr	-72.7	-22.7	-56.7	-42.1	3.19/3.21	-10.2
Ti-6Mo-5Nb-3Zr	-69.1	-27.1	-57.1	-42.7	3.23/3.26	-8.61
Ti-6Mo-4Nb-4Zr	-48.9	-28.8	-48.9	-38.9	3.24/3.29	-8.1

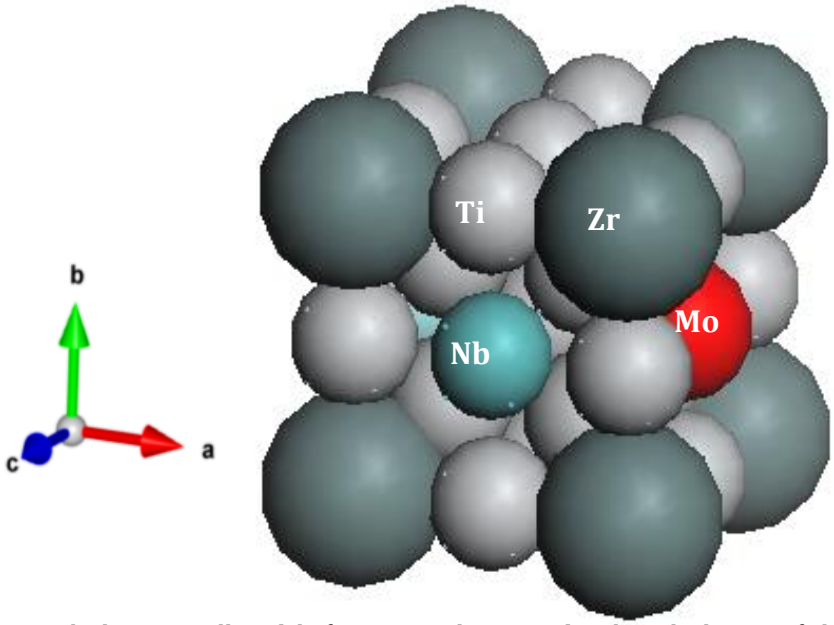

Fig. 1: *The bcc unit cell model of Ti-6Mo-xNb-xZr used in the calculations of elastic coefficients. Here Ti and Mo atoms are shown in grey and deep green, while Zr and Nb are represented in red and lighter green respectively.*

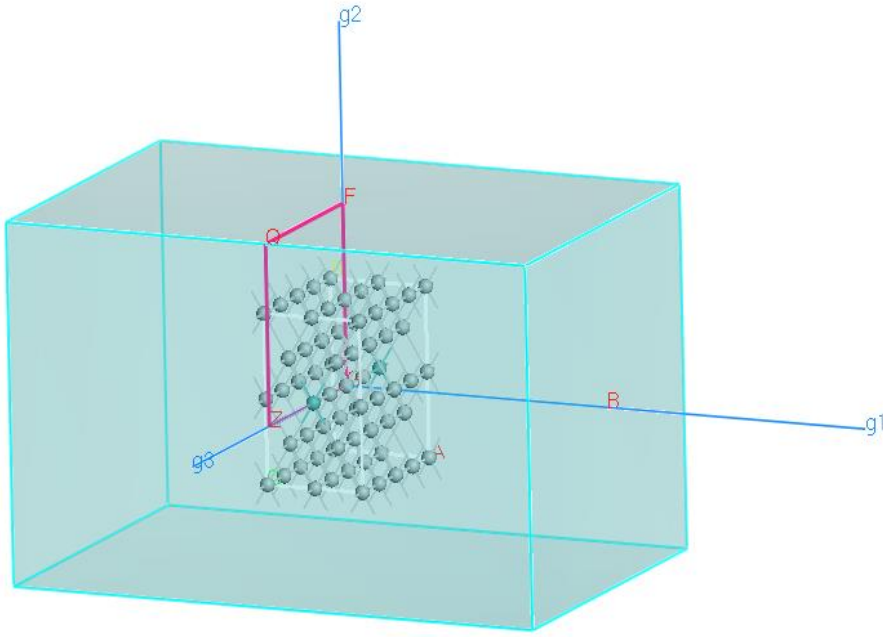

***Fig. 2**: Layer slab super cell for (110) surface energy and elastic matrix*

From the view point of thermodynamic stability, for an alloy to be thermodynamically stable, its formation energy must be negative. We apply this criterion to study the energetic influence of alloying element on the structural stability. The calculated results of the effect of Nb and Zr micro-additions on the formation energy E_{Fm} (meV/atoms,), cohesive energy(E_c) (meV/atom) and lattice constant, a (Å) for the various phases are listed in Table 1. The lattice constants of the structures are calculated by geometrical optimization. As seen in Table 1. the alloying elements considered here are good β stabilizers, as the values of the formation energies E_{Fm} for β(bcc) phase are more negative than those of ω, α and α′′ phases. From this perspective, we can infer that the synergic additions of Nb and Zr elements in the alloy destabilize the ω and α phases (their formation energy increases with the composition x) but stabilize the α′′ and β-phase (their formation energy decreases with composition x). It is notable that orthorhombic α'' phase and bcc β phase exhibited similar stability trend with close values of formation energies,E_{Fm}, however, the values for the β (bcc)-phase is lower than that of the α′′ phase. This implies that the ternary and quaternary addition of Nb, Zr or their synergic micro-alloying additions are energetically favourable to stabilising the β-phase with low composition (<6at. %) in the Ti-Mo alloy.

Similarly, from the values of the cohesive energy (E_c) shown in Table 1, the β-stability of the alloys can be ranked in the order: Ti-6Mo-6Nb> Ti-6Mo-6Nb-2Zr> Ti-6Mo-5Nb-3Zr> Ti-6Mo-4Nb-4Zr> Ti-6Mo-6Zr. The present results are consistent with other first principles calculations [44, 45, 46] as well as previous experiment phenomena [13]. Some of this trend was confirmed experimentally, as explained below

In view of the practical use of the alloys for implant application in human body, T= 310K is a suitable reference for the study of relative stability of the alloys. In order to determine the thermodynamic properties and stability of phases at this temperature, the entropy effects were considered. These can be decomposed for solids into a configurational (mixing) and vibrational contribution [37]. In this study we use a rough estimate of the temperature dependence and neglect the vibrational contribution which is computationally difficult to access. The remaining contribution, the configurational entropy, is calculated in the ideal mixing approximation. This approximation becomes exact for alloys where the formation energy depends only on the concentration, not on the local atomic configuration, which was of no effect.

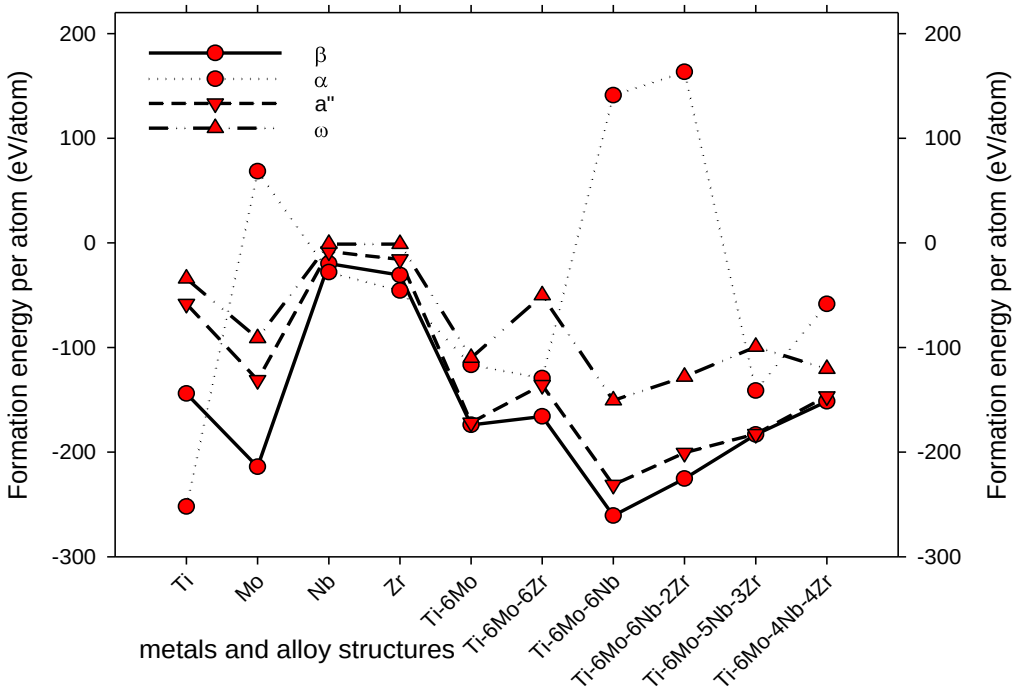

Fig. 3*: Theoretical formation energies of Ti-6Mo-xNb-xZr alloys (where x= 0, 6, 6, 5 and 4 at. % for Nb and x= 6, 0, 4, 3 and 2 at. % for Zr) as a function of x concentration at T=3310K. The lines are for eye guidance.*

Table 2: The chemical compositions of the Ti-6Mo-Nb-Zr alloys studied by EDXRF (at a resolution near 150 eV FWHM (all in atomic %).

Materials	Mo	Nb	Zr	C	Cu	Si	O	H	Ti
Ti-6Mo6Zr	5.98	5.93	5.96	0.018	0.005	0.011	0.045	0.0036	Bal.
Ti-6Mo-6Zr	5.98	5.93	5.96	0.018	0.005	0.011	0.045	0.0036	Bal.
Ti-6Mo-6Nb	5.97	5.96	2.97	0.010	0.003	0.011	0.045	0.0036	Bal.
Ti-6Mo-5Nb-3Zr	5.98	4.99	2.97	0.02	0.002	0.012	0.044	0.0036	Bal.
Ti-6Mo-4Nb-4Zr	5.97	3.96	3.98	0.001	0.003	0.010	0.045	0.0036	Bal.

As shown below, the approximation is well justified in the case of the Ti alloys studied here. The ideal mixing entropy is given by:

$S_{conf(x)}=K_B[x.In(x)+(1-x).In(1-x)]$ (10)

where x is the alloy composition of a multicomponent alloy $Ti_xMo_6\,Nb_xZr_x$ and K_B is the Boltzmann constant. The temperature dependent free energy can then be calculated according to:

$F_r(x,T)=\langle E_F(Ti-6Mo_xNb_xZr)\rangle - TS_{conf.}$ (11)

where the averaged formation energy of $Ti-6Mo_xNb_xZr$ alloys is obtained from the formation energies of alloys with different local atomic configuration, but same concentration by averaging using the Boltzmann statistics at the reference temperature. The temperature-dependent free energy of formation allows us to determine the thermodynamic stability of an alloy at a given temperature. The corresponding results are shown in Fig. 3. Although the effect of temperature is less pronounced, evidently the finite temperature significantly reduced the formation energy, which implies that the stability of the alloy is somewhat entropy driven.

Comparing the (E_{Fm}) curves for the different crystal structures, we can infer that (bcc) β-type phase is the most stable phase, while the (α′′) orthorhombic-type phase is likely a metastable phase at the reference temperature. Therefore, the elastic modulus of the alloys was modelled as a polycrystalline aggregate of α′′/β composite in the alloy matrices.

The experimental verification of the trend obtained from the theoretical formation energy is presented in the preceding section.

3.2 Comparison with experimental data: Composition and Phase analyses

Chemical analyses (EDXRF) were performed in many different areas (bulk and surface), and results show that the actual chemical composition of the alloys is close to nominal values (See Table 2), agreeing with ASTM F-67. As can be seen, all the alloys are within ~±1% variance when the experimental and nominal values were compared. The chemical composition of the alloys was homogeneous and no expressive differences were found between the bulk and surface of the samples, which indicates a good homogenisation of the studied alloys. In order to elucidate the compositional sensitivity of alloy elements in the Ti-Mo alloy system, an XRD analysis was carried out at room temperature on solution treated (designated as ST) and swaged plus annealed (SW) specimens.

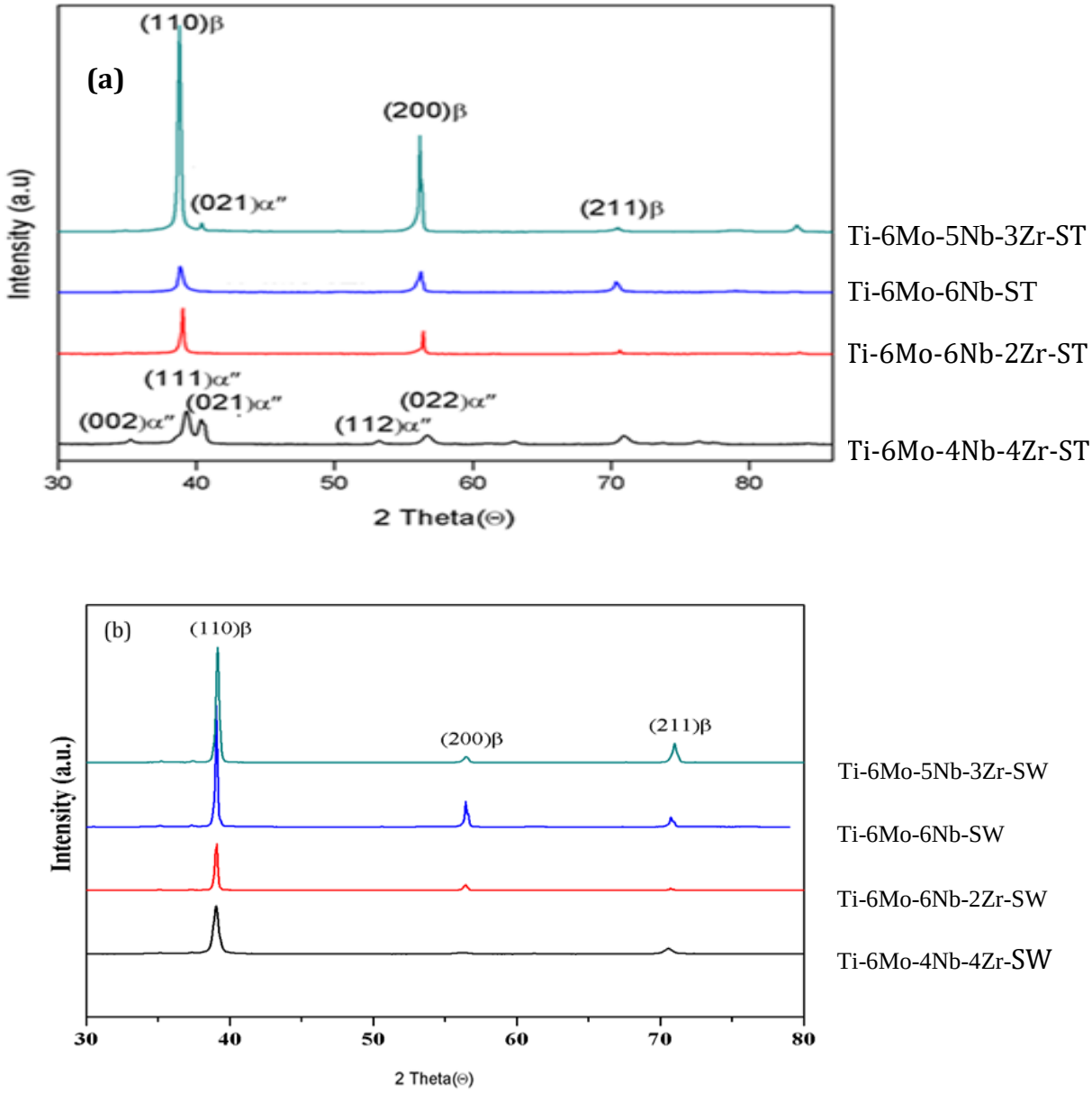

***Fig. 4**: XRD profiles of Ti-6Mo-xNb-xZr alloys (where x= 0, 6, 6, 5 and 4 at. % for Nb and x=6, 0, 4, 3 and 2 at. % for Zr) subjected to (a) solution treatment (ST) and (b) Swaged and(SW)*

The XRD results for ST and SW samples scanned from 30 to 80 degrees in diffraction angle (2θ) are presented in Fig. 4(a) and (b) respectively. Fig. 4(a) provides unambiguous evidence for the presence of the β phase in all alloys after solution treatment at 1073K for 1hour followed by quenching into water, thus confirming the sensitivity of the initial binary Ti-6Mo alloy to the micro-additions (Nb and Zr). Strong β peaks associated with the (002), (200), (220) and (211) diffraction planes are evident in all the samples. When comparing the results of the different alloy samples, the diffraction peaks of orthorhombic α′′ were detected in Ti-6Mo-5Nb-3Zr-ST and Ti-6Mo-4Nb-4Zr-ST specimens, as indicated by the splitting of the single α′ (1010) peak into three α′′ peaks. These α′′ peaks are of a much weaker intensity, or unnoticed, in the other alloys. This is consistent with the theoretical data; besides the Ti-6Mo-6Zr alloy consisting of no Nb, Ti-6Mo-4Nb-4Zr and Ti-6Mo-5Nb-3Zr alloys have the least negative formation energy and cohesive energy values. According to various references [20,21,22], the amount of α′′ martensite phase in Ti alloys is conditioned by the β-stabiliser content and by grain size. When Nb is low, there exists an orthorhombic α′′ phase, but when Nb is high, the α′′ phase peaks become weaker and more diffuse. In line with this finding, α′′ (020), α′′ (111) and α′′ (021), α′′ (022), α′′ (131) and α′′ (221) peaks exist in the Ti-6Mo-4Nb-4Zr-ST sample. A weaker and more diffused α′′ (021) peak appeared in the Ti-6Mo-5Nb-3Zr –ST sample, while just a single β phase exists in the Ti-6Mo-6Nb-ST and Ti-6Mo-6Nb-2Zr-ST alloys (consisting of high Nb contents). Clearly, with the Nb content increasing, the β phase becomes stable. The diffraction peaks of the α′ or ω phases have not been detected, although the intensity of ω phase is not always high enough to provide evidence of the presence of ω phase when the ω phase has quite a small size or volume fraction. However, the results are in good agreement with the theoretical data. Interestingly, upon SW at 673K for 20 minutes, the α′′ vanishes in the XRD profile of all the samples as shown in Fig.4 (b). Strong β peaks associated with the (002), (200), (220) and (211) diffraction planes are evident in all the SW specimens without any trace of a metastable phase. This suggests that α′′ phase is formed before it transformed back to β phase upon annealing.

β-transus for pure Ti is reported at 882 °C and the addition of β stabilizing element reduces this value. It is known that, under the Ti-Mo binary system, Mo or any other β stabilizing elements lowers the β transus and promotes the formation of the β phase, while also suppressing other metastable alloys , such as ω, α and α′′ at room temperature. Therefore, DTA was used to characterise the β transus of the ST specimens from 0 to 1200°C during heating and cooling, and the results are shown in Fig. 5. Obviously, it can be seen that it was only in low or none Nb containing alloys (Ti-6Mo-6Zr and Ti-6Mo-4Nb-4Zr) that exothermic peaks were found at 861K (588°C). When comparing the results of the different alloy samples, it is clearly evident that with the Nb content increasing, the β phase becomes stable, lowering β transus temperature below room temperature, thus suggesting that the β to α′′ martensitic transformation can be effectively retarded or even suppressed by specific alloying and subsequent heat treatment. This result is consistent with the result obtained from the theoretical data.

3.2. Comparison with experimental data : Mechanical property

As mentioned before, when elastically soft bone tissue is replaced by a stiffer implant, the implant takes over a considerable amount of the load, shielding the surrounding parts of the skeleton. Reducing the physiological loads on the bone induces re-sorption processes that give rise to a drop in bone density, mineralization state and strength [25]. Stress shielding can finally promote contact loosening, implant failure, or debris-induced infections. Therefore, it is of great importance that the elastic mismatch between the bone replacement material and existing bone be minimized in metallic biomaterials intended for orthopaedic application.

Table 3: Theoretically predicted polycrystalline integral elastic parameters and phase composition of multicomponent Ti-Mo composites with selected Nb and Zr concentrations (of actually cast samples) together with the experimental data of Ti, Nb, Zr, Mo and other multicomponent Ti-6Mo alloy.at zero pressure.

Material	Elastic properties (GPa) and phase composition together with the experimental data.								
	V_{β}^{Theor}	V_{β}^{Exp}	$B_{\beta/\alpha''}$	$G_{\beta/\alpha''}$	$E_{\beta/\alpha'}^{Theory}$	$E_{'[ST]}^{Exp.}$	$E_{'[SW]}^{Exp.}$	$\upsilon_{\beta/\alpha''}$	G/B
αTi	0	0	111.3	39.4	131.6	-	-	0.33	0.35
Mo	1	1	120.3	22.5	113.3	-	-	0.37	0.6
Nb	1	1	136.3	58.6	150.8	-	-	0.31	0.43
Zr	0	0	103.2	60	93.0	-	-	0.36	0.58
Ti-6Mo	0.29	0.31	101.2	41	102.1	96.5	117	0.24	0.41
Ti-6Mo-6Zr	0.18	0.22	190.73	49.2	70.2	65.2	71.3	0.26	0.42
Ti-6Mo-6Nb	0.78	0.73	100	42.18	90.6	77.7	81.4	0.18	0.26
Ti-6Mo-6Nb-2Zr	0.67	0.61	114.83	40.46	76.5	58.7	73.5	0.19	0.30
Ti-6Mo-5Nb-3Zr	0.58	0.53	118.2	46.12	59.1	61.3	76.1	0.20	0.32
Ti-6Mo-4Nb-4Zr	0.42	0.39	104.1	49.6	38.3	41.02	54.0	0.20	0.35

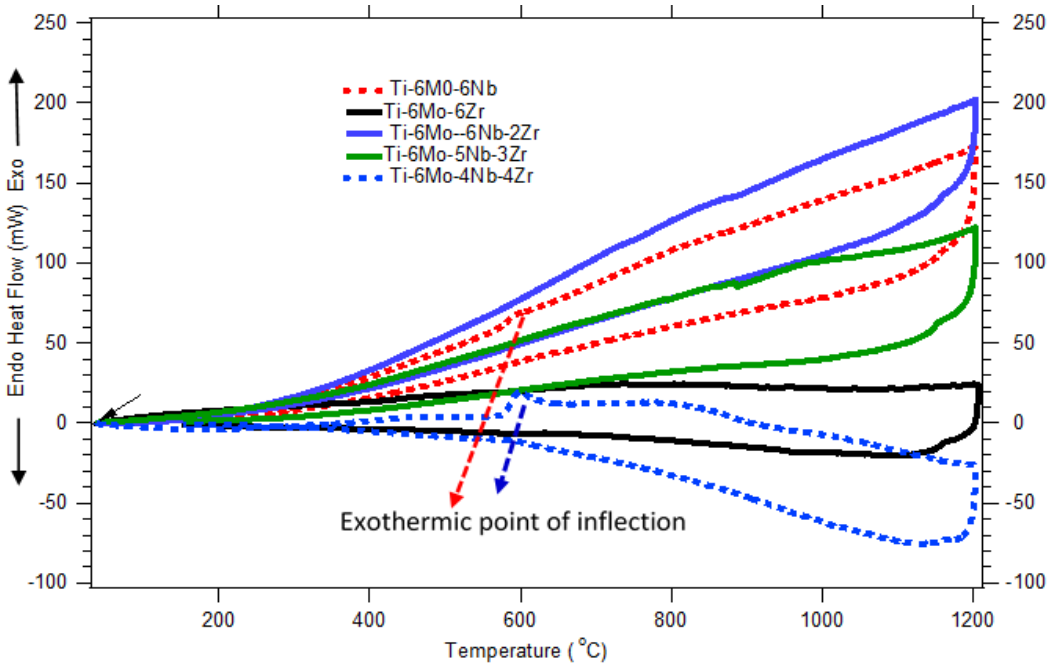

Fig. 5: comparison of the DTA patterns of Ti-6Mo-xNb-xZr alloys (where x= 0, 6, 6, 5 and 4 at. % for Nb and x= 6, 0, 4, 3 and 2 at. % for Zr).

In this study, the elastic response for each condition was evaluated by ultrasonic technique to measure the change in the Young's modulus of the alloys, and compared with theoretical data. The test was performed for at least five times before taking an average value.

3.2.1 Elastic modulus: Theory and Experiment

Taking into account the structure symmetry and the volumetric fraction of phase components, the polycrystalline elastic modulus was computed by homogenizing the elastic properties of the polycrystalline α′′/ β composite using Eqns. 3-9 to determine the Young's modulus$(\tilde{E})^{*}$, Poisson's ratio$(\upsilon)^{*}$, Bulk modulus (B) and Shear modulus (G).

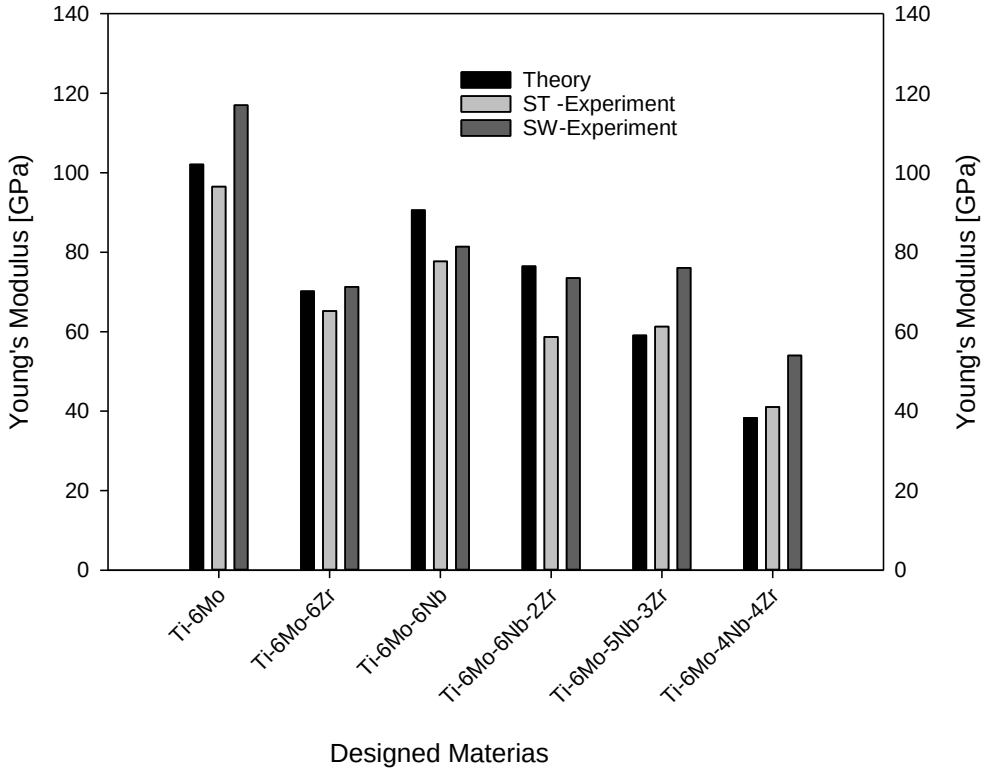

Fig.6*: Theoretical calculated Young's modulus, E of Ti-6Mo-xNb-xZr (x= 0, 6, 6, 5 and 4 at. % for Nb and x= 6, 0, 4, 3 and 2 at. % for Zr) compared with data from experimental result.*

The theoretically predicted elastic material properties compared with experimental data obtained in this study are summarized in Table 3 and visualized in Fig.6. Fig. 6 shows the Young's moduli of the multicomponent Ti-6Mo –XNb-xZr alloys subjected to solution treatment (ST) and swaging (SW) (process described earlier). All the alloys subjected to solution treatment exhibit considerable low Young's moduli of <75GPa which is much less when compared with those of SUS 316L, CP-Ti and Ti64 ELI [7]. In the latter case, the values are generally high. For the ST samples, the trend depicted in the figure shows that as the Nb increases, the Young's modulus increases. The result indicates elastic moduli values of 60.2GPa, 74.7GPa, 68.7GPa, 61.3GPa, and 41.02GPa for Ti-6Mo-6Zr,Ti-6Mo-6Nb,Ti-6Mo-6Nb-2Zr,Ti-6Mo-5Nb-3Zr and Ti-6Mo-4Nb-4Zr alloy samples, respectively, with an estimated error of ±3%, which represents ~ 41% reduction in the Young's modulus of Ti-6Mo alloy(See Table 3). The latter indicates 71.3 GPa, 81.4 GPa, 73.5GPa, 77.1 GPa, and 54.0GPa for Ti-6Mo-6Zr, Ti-6Mo-6Nb, Ti-6Mo-6Nb-2Zr, Ti-6Mo-5Nb-3Zr and Ti-6Mo-4Nb-4Zr alloy samples, respectively (for the SW samples).

It is well known that phase(s) as the main constituent of microstructure has a significant effect on the mechanical properties of Ti alloys [31] and that is likely to increase or decrease the Young's modulus. Therefore the presence of a single β-phase in the SW samples (Fig.4b) is the main factor in the change in Young's modulus among the designed alloys.

As evidenced in Table 3 and visualized in Fig. 6, our theoretical result agrees well with the experimental (ST) values within an error margin of ~±2%. It can be recalled that both the theory (Fig. 3) and experiments (XRD and DTA analyses) in Figs. 4 (a) and (b), and 5 indicate that the two alloys that exhibit the lowest Young's moduli (Ti-6Mo-5Nb-3Zr and Ti-6Mo-4Nb-4Zr) had α″ orthorhombic martensite phase in their matrix. Thus, their

low E can be ascribed to the presence of the α′′ plates, which presents a modulus about half of that of the β phase [30]. The small discrepancies in the results could reflect differences in temperature, minor experimental errors or the approximations inherent in DFT-GGA [18, 30]. Therefore, it is apparent that the technique of coupling the elastic properties by homogenising multiphase elastic parameters may lead to something of a breakthrough with respect to reducing the Young's modulus of metallic biomaterials.

Poisson's ratio (ν) provides more fundamental information about the characteristics of the bonding forces than any other elastic constants [38]. The 0.25 and 0.5 are the lower and the upper limits for central force solids, respectively [39]. Our theoretical result of the Poisson's ratio of the designed alloys is in the range of 0.18 and 0.22, which shows that bonding forces are non-central forces and the lower the Nb, the more the directional bonding in the multicomponent Ti-6Mo-xNb-xZr alloys studied. Moreover Poisson's ratio shows relation with the iconicity of compounds [38]. It has a small value (ν=0.1) for covalent materials and has a typical value of (ν=0.25) for ionic materials. In our case, the Poisson's ratio shows that they mainly exhibit covalent characteristics. The addition of Nb and Zr alloy elements led to low Poisson's ratio, and improved bonding covalency.

Similarly, whether or not a material demonstrates brittle or ductile behaviour is of central importance as it has a direct influence on its applications range. From this perspective, Pugh [27] proposed the ratio of bulk to shear modulus of materials, B/G ratio as an indication of brittle and ductile behaviour: low G means low resistance to shear, hence ductility while low B means low resistance fracture, hence brittleness. The critical value which separates ductile and brittle materials has been evaluated to be equal to 1.75. If B/G>1.75, a material behaves in a ductile manner, and vice versa, if B/G <1.75, a material demonstrates brittleness. From the theoretical data shown in Table 3, all the designed Ti-6Mo-xNb-xZr alloys exhibited good ductile behaviour. Therefore, *B/G* can describe the brittle/ductile properties of materials, and understanding these differences is essential in analysing the mechanical properties of materials with different slip characteristics.

3.2.2 Hardness

The result of Vickers hardness measurement of the multicomponent Ti-6Mo–XNb-xZr alloys subjected to solution treatment (ST) and swaging (SW)plus anneal are listed in Table 4 and they are very similar to those of other biomedical Ti alloys with Nb and Zr additions.

Table 4: Mechanical properties of designed multicomponent Ti-Mo alloys and some typical metallic biomaterials

Materials	**Hardness -ST [HV]**	**Hardness -SW [HV]**	**Yield Strength [$\sigma_{0.2}$ (MPa)]**
CP –Ti[22]	297.76	-	170-485
Ti-6Al-4V[22]	325.87	-	825-869
ASTMF75[ ](Co-Cr-Mo)	354.9	-	448
Ti-10Mo [22]	325.3	-	412
Ti-15Mo [22]	342.8	-	544
Ti-20Mo [22]	358	-	428
Ti-6Mo [this work]	298	346	483
Ti-6Mo-6Zr [this work]	301	341	-
Ti-6Mo-6Nb [this work]	324.13	363	-
Ti-6Mo-6Nb-2Zr [this work]	326.98	360	-
Ti-6Mo-5Nb-3Zr [this work]	322.7	347	-
Ti-6Mo-4Nb-4Zr [this work]	305	345	-

For example, Vickers Hardness Values of Ti-10Mo-xNb alloys(x=3, 7, 10) were between 396 and 441 HV [13], while those for alloys in Ti-8Mo-xZr system were between 400 and 500HV [7]. For the SW specimens, it is notable that alloys that exhibit α″ orthorhombic martensitic phase (Ti-6Mo-6Zr-ST and Ti-6Mo-4Nb-4Zr-ST) possess significantly lower hardness values (≈301-305 HV), while the hardness of the specimens consisting of single β phase (i.e., Ti-6Mo-6Nb-ST and Ti-6Mo-6Nb-2Zr-ST alloys) are 324.13HV and 326.98 HV, respectively. The highest value compares very well with the hardness 325.87 HV of solution-treated Ti-6-4 alloys (i.e Ti-6Al-4V alloys) that have been accepted by the bio-implant research community as a material of choice. Generally, this can be attributed to two factors: the first is the higher solid solution effect, precipitation hardening exhibited by β phase due to increasing Nb concentration. The other can be linked to the grain size exhibited by the samples.

As envisaged, the hardness values of the SW specimens are higher than those of the ST specimens (See Table 4). This change in hardness of the SW alloys is attributed to the increase in strength during the deformation process. This promotes the development of small grain size, small grain boundaries and high dislocation density. According to the Hall-Petch principle, this should result in high strength and hardness values in the SW designed multicomponent alloys. The hardness value for the specimens are 346HV, 341HV, 363HV, 360HV, 347 HV, 345 HV for Ti-6Mo,Ti-6Mo-6Zr , Ti-6Mo-6Nb,Ti-6Mo-6Nb-2Zr , Ti-6Mo-5Nb-3Zr and Ti-6Mo-4Nb-4Zr, respectively.

4.0 CONCLUSIONS

A multidisciplinary approach was used to predict the polycrystalline phase stability, elastic constants and electronic properties of five dual-phase multicomponent Ti-6Mo alloys. The approach combines a thermodynamic analysis with a self-consistent homogenization scheme that can describe phases with differing crystal structures. Thermodynamics provides the composition and volume fraction of the various phases, while homogenization estimates polycrystalline elastic constants from single crystal ones. All of the input values for this multi-scale approach originate from ab initio calculations, making this approach a strong tool in a theory-guiding materials-design strategy.

In this study, the thermodynamic analysis predicts the volumetric fraction of bcc-β phase composition in the alloys and the results is in good agreement with experimentally measured data. The composite is predicted to consist of mainly cubic β-phase with fairly high Nb content (~ 6at. %). Despite the fact that our theoretical thermodynamic analysis overestimates the volume fractions of β phase compared with those experimentally found, the predicted compositional trend is qualitatively correct.

The resulting Young's modulus of polycrystalline α/β Ti-Mo alloys decreased as the volume fraction of α′′phase (or Nb content) decreased. Theoretically, a complete suppression of the presence of α′′phase would result in a reduction of the Young's modulus to about 38 GPa, which is predicted in the case of dual α′′ and β-Ti-6Mo phase containing 4at. % Nb and 4at. % Zr, respectively. While the predicted modulus values are generally lower than that experimentally observed, the compositional trends are predicted correctly. From an alloy design perspective, we can conclude that in order to achieve maximum softness, the amount of the orthorhombic α′′-phase should be optimized via keeping the amount of Nb low enough to ensure thermodynamic stability of the α′′ in β-Ti-Mo.

REFERENCES

1. M. Long, H.J.Rack, Biomaterials 19 (1998) 1621–1639.

2. M. Niinomi, Mater. Sci. & Eng A 243 (1998) 231–236.

3. S. Ankem S, CA. Greene Mater Sci Eng A 263(2) (1999), 127. doi: 10.1016/S0921-5093(98)01170-8

4.. M. Niinomi, Sci Technol Adv Mater 4 (2003), 445. doi:10.1016/ j.stam.2003.09.002

5. P.S.Nnamchi, I Todd and M.W. Rainforth, PhD Thesis, Department of Materials Science and Eng., University of Sheffield, Uk, (2014).
6. Y. Okazaki, S. Rao, Y. Ito, T. Tateishi, Biomaterials 19 (1998) 1197–1215.
7. K. Wang Mater Sci Eng A 213 (1996) 1–2:134. doi:10.1016/ 0921-5093(96)10243-4
8. J. Black and G. Hasting: Handbook of Biomaterials Properties, Chapman and Hall, London, (1998), 167–98.
9. ASM Handbook, vol. 2, Properties and Selection: Nonferrous Alloys and Special-Purpose Materials, Joseph R. Davis, ed., ASM INTERNATIONAL, Materials Park, OH, (1990), 3–15.
10. YL Hao, Li SJ, Sun SY, Zheng CY, Hu QM, Yang R (2005) Appl Phys Lett 87(9):091903. doi:10.1063/1.2037192
11. M. Abdel-Hady, K. Hinoshita, M. Morinaga, Scripta Mater 55-5, (2006), 477. doi:10.1016/j.scriptamat.2006.04.022
12. D. Eylon, RR. Boyer, DA. Koss, Beta titanium alloys in the 1990s. Minerals, Metals & Materials Society (1993), New York
13. C. Zhang, H. Tian, C. Hao, J. Zhao, Q. Wang, E. Liu and C. Dong, J Mater Sci 48 (2013) 3138–3146: DOI 10.1007/s10853-012-7091.
14. D. Raabe, B. Sander, KM. Fria, D. Ma and J. Neugebauer, Acta Mater 55-13 (2007), 4475. doi:10.1016/j.actamat.2007.04.024.
15. H. Ikehata, N. Nagasako, T. Furuta, A. Fukumoto, K. Miwa,T. Saito Phys. Rev.B 70-17, (2004),174113.doi:10.1103/PhysRevB.70.174113.
16. Ho W. F., Ju C. P. and Lin J. H., Biomaterials 20 (1999), 2115-22.
17. L. Trentani, F. Pelillo, F.C. Pavesi, L. Ceciliani, G. Cetta, A. Forlino, Biomaterials 23 (2002) 2863–2869.
18. D.M. Gordin, T. Gloriant, G. Texier, I. Thibon, D. Ansel, J.L. Duval, M.D. Nagel, J, Mater. Sci.: Materials in Medicine 15 (2004) 885–891.
19. S. Nag, R. Banerjee, H.L. Fraser, Mater. Sci.& Eng. C 25 (2005) 357–362.
20. K. Rajamallu, M. K. Niranjan and S.R.Dey, Mater. Sci. &Eng.C 50(2015) 52–58
21. I.J. Polmear, Light Alloys From Traditional Alloys to Nanocrystals, 4th ed., Elsevier, (2006), 301.
22. S.J.Clarck, M.D.Segal, C.J.Pickard, P.J.Hasnip, M.J.Probert, K.Refsen, M.C.Payne. Z.Krystallogr. 220(2005) 567.
23. M.D.Segal, P.J.D.Lindan, M.J.Probert, C.J.Pickard, M.C.Payne. J. Phys: Condens Matter 14 (2002) 2717.
24. W.Kohn, L.J.Sham. Phys. Rev. A 140(1965) 1133.
25. M.C.Payne., M.P.Teta, D.C.Allen, T.A.Arias, J.D.J.Joannopoalos. Rev. Mod. Phys. 64(1990) 1045.
26. J.P.Perdew, J.A. Chevary, S.H.Vosko, K.A.Jackson, M.R.Pederson, D.J.Snigh, C. Fiolhais. Phys. Rev.B. 46(1992) 6671.
27. H.J.Monkhorst, J.D.Pack. Phys. Rev.B. 13 (1970) 5188.
28. M. Abdel-Hady, K. Hinoshita, M. Morinaga, Scripta Mater 57 (2007), 1000-1003.
29. O. Eriksson, Encyclopaedia of Materials: Science and Technology, Elsevier, Amsterdam, (2003), 1–11.
30. B.V. Beznosikov, J. Struct. Chem. 44 (2003) 885.
31. R. Zeller, P.H. Dederichs. *Phys. Stat. Solid. B* 55 (1973) 831–842.
32. T.R. Middya, A.N. Basu. *J. Appl. Phys. 59(*1986), 2368–2375.
33. T.R. Middya, M.Paul, A.N. Basu, *J. Appl. Phys. 59(*1986), 2376–2381.
34. D. Raabe, B. Sander, M. Friak, D. Ma, J. Neugebauer. *Acta Mater. 55, (*2007) 4475–87.
35. Ho W. F, Ju C. P. and Lin J. H., Biomaterials 20 (1999), 2115-22.
36. W.A. Counts, W.A, M. Friak, D. Raabe, J. Neugebauer. *Acta Mater. 57(*2009), 69–76.
37. W.A. Counts, W.A, M. Friak, D. Raabe, J. Neugebauer. *Adv. Eng. Mat. 12(*2010), 572–76.
38. J.F. Nye, Propriétés Physiques des Matériaux, Dunod, 1961.
39. M. Born and K. Huang, Dynamical Theory of Crystal Lattices (Boxford, Clarendon, 1954), 336–8.
40. V. Milman, M.C. Warren, J. Phys.: Condens. Matter 13 (2001) 241.
41 J. Wang, S. Yip, S.R. Phillpot, D. Wolf, Phys. Rev. Lett. 71 (1993) 4182.
42. B.V. Beznosikov, J. Struct. Chem. 44 (2003) 885.
43 S.F. Pugh, Philos. Mag. 45 (1954) 823.
44. J. H. Dai, X. Wu, Y. Song, and R. Yang. J. App. Phy. 112,(2012) 123718.
45 A. D. Becke and K. E. Edgecombe, J. Chem. Phys. 92, 5397 (1990).

46. A. Savin, R. Nesper, S. Wengert, and T. F. F€assler, Angew. Chem. Int. Ed. Engl. 36, 1808 (1997).

47. R. F. W. Bader, Atoms in Molecules: A Quantum Theory (Oxford University Press, New York, 1990).